Quasi-decadal and inter-decadal climate fluctuations in the Pacific Ocean from a CGCM

Yves M. Tourre,[1,2] Carole Cibot,[3] Laurent Terray,[4] Warren B. White,[5] and Boris Dewitte[6]

Received 25 November 2004; revised 2 February 2005; accepted 4 March 2005; published 15 April 2005.

[1] Diagnostic analyses in the Pacific, have revealed distinct quasi-decadal (QD) and inter-decadal (ID) climate fluctuations with coherent varying patterns of sea surface temperature (SST) and sea level pressure (SLP) anomalies. From a 200-year CGCM simulation, distinct low-frequency fluctuations are also obtained: QD (i.e., 8–12 years period band) and ID (i.e., 18–25 years period band). Traced modeled QD evolution reveals equatorial SST anomalies resembling ENSO, while tropical recharge/discharge mechanisms seem to be operating. The traced modeled ID evolution reveals high latitudes spatially coherent patterns, with maximum SST anomalies in the vicinity of the subarctic frontal zone (SAFZ) and subtropical gyres through advection. Contrary to QD SST anomalies, the modeled ID SST anomalies peak away from the equator as observed. QD fluctuations may then be viewed as low-frequency ENSO phenomena, while ID fluctuations may set-up thermal background modulating frequency and intensity of ENSO. **Citation:** Tourre, Y. M., C. Cibot, L. Terray, W. B. White, and B. Dewitte (2005), Quasi-decadal and inter-decadal climate fluctuations in the Pacific Ocean from a CGCM, *Geophys. Res. Lett.*, *32*, L07710, doi:10.1029/2004GL022087.

1. Introduction

[2] Low-frequency oscillation, defined as PDO [*Mantua et al.*, 1997], does not provide distinction between QD and ID climate fluctuations. Besides secular and multi-decadal scales variability, low-frequency climate fluctuations in the Pacific Ocean include two co-varying SST and SLP anomalies (SLPA and SSTA), with QD and ID time scales (i.e., 8-to-12 years and 18-to-25 years period bands). These two fluctuations have distinct spatial evolutions that must invoke different physical mechanisms, to propagate against dissipation [*Liu*, 1999; *Tourre et al.*, 1999, 2001]. Some aspects of these fluctuations have been modeled (i.e., *Pierce et al.* [2001], *Qiu* [2003] for QD, *Miller and Schneider* [2000], *Auad* [2003], and *Latif and Barnett* [1994] for ID). QD fluctuations require coupled Rossby wave dynamics providing a delayed-negative feedback mechanism that gives the signal its characteristics [*White et al.*, 2003]. ID fluctuations require a gyre adjustment for a reddening of the spectrum of ocean climate variability [*Seager et al.*, 2001]. Both fluctuations are associated with near-stationary atmospheric winter spatial patterns, with significant drought and wet spells across North America [*L'Heureux et al.*, 2004].

[3] Other distinct features between the two fluctuations exist. For the QD signal, high latitudes SLPA and SSTA develop together with same polarity. For the ID signal, the development of SLPA in the North Pacific which occur well before the development of SSTA to the southwest with same polarity, could be forced by enhanced convection in the tropics and teleconnected patterns [*Kachi and Nitta*, 1997]. Extreme values of a deeper Aleutian low could enhance the subpolar gyre [*Sekine*, 1988], with extreme values of SSTA appearing ~3 years later, in the vicinity of the SAFZ in the Northern Hemisphere. Through subtropical gyres evolutions, tropical SSTA then reach maxima in the central Pacific and away from the equator near 15° latitudes (Northern and Southern Hemispheres). The latter anomalies must modify the tropical ocean thermal background, the atmospheric SLP large scale patterns, and contribute to modulations of the intensity and evolution of ENSO [e.g., *Kirtman and Schopf*, 1998; *Yeh and Kirtman*, 2004].

[4] In this paper, the joint low-frequency variability of SSTA and SLPA in the Pacific Ocean is analyzed from a 200-year climate global coupled-model (CGCM) run at the European Centre for Research and Advanced Training in Scientific Computation (CERFACS). Results are compared with those obtained from diagnostic studies while some mechanisms are proposed. A better understanding of the dynamics of low-frequency climate fluctuations may yield considerable regional predictive capabilities and shed some light on climate change.

2. Data and Methods

[5] Data is from a CGCM using the OASIS3 CERFACS coupler: The ocean component, ORCA2 (including sea-ice) has been developed at the Laboratory of Ocean Dynamics and Climatology (LODYC), while the atmospheric component, ARPEGE-Climat has been developed at the 'Centre National de Recherches Météorologiques' (Météo-France). For detailed description of the physics of the CGCM see *Cibot et al.* [2005]. In order to compare model output with those from diagnostic studies, global and monthly SSTA and SLPA from the model are interpolated on the Kaplan grid-point systems [*Kaplan et al.*, 1998], to form subsets of data for the Pacific domain (60°N–30°S), on 5° × 5° and 4° × 4° grids. The Multi Taper Method/Singular Value

[1] Mediterranée et Afrique Subtropicale–France (MEDIAS-France), Centre National d'Etudes Spatiales, Toulouse, France.
[2] Lamont-Doherty Earth Observatory of Columbia University, Palisades, New York, USA.
[3] Météo-France, Toulouse, France.
[4] Centre Européen de Recherche et de Formation Avancée en Calcul Scientifique (CERFACS), Toulouse, France.
[5] Scripps Institution of Oceanography, University of California San Diego, La Jolla, California, USA.
[6] Laboratoire d'Etudes en Géophysique et Océanographie Spatiales (LEGOS)/Institut de Recherche Pour le Développement (IRD), Toulouse, France.

0094-8276/05/2004GL022087$05.00

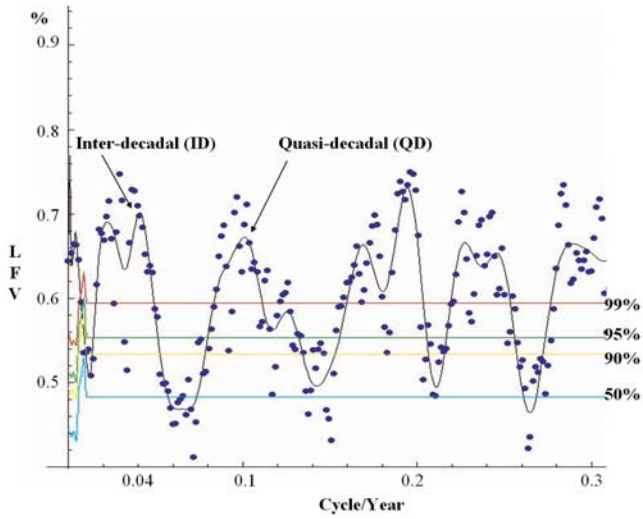

Figure 1. Local Fractional Variance (LFV) for joint SSTA-SLPA analysis, using MTM/SVD. Blue dots are joint LFV values prior to smoothing. Thin black line is obtained from polynomial smoothing. Peaks for Inter-decadal and Quasi-decadal are highlighted. Horizontal lines represent Monte Carlo significance levels. Cycle/year on abscissa.

Decomposition (MTM/SVD) is used [*Mann and Park*, 1999]. The chosen time-frequency bandwidth is based upon three tapers for reasonable low-frequency resolution and sufficient degrees of freedom for a proper signal/noise ratio. The joint local fractional variance (LFV) spectrum represents 'joint signal power' in relatively narrow frequency bands associated with coherent spatio-temporal fluctuations (see *Mann and Park* [1999] for further details).

3. Results

[6] From the model run, inter-annual variability is identified within two period bands: 2-to-3 years, and 3-to-8 years. Within the 2-to-3 years band (i.e., quasi-biennial fluctuations, not shown) SSTA peaking at the equator are larger than observed. The modeled over-energetic variability in the quasi-biennial band is due to biases in the seasonal cycles favoring high-frequency signals similar to ENSO (B. Dewitte et al., Role of equatorial background mean state and near-annual coupled mode in a CGCM simulation, submitted to *Journal of Climate*, 2004, hereinafter referred to as Dewitte et al., submitted manuscript, 2004). In this paper only the low-frequency part of the LFV spectrum (i.e., minus the quasi-biennial frequencies) is displayed in Figure 1.

[7] Significant and separated frequency bands are obtained: three ENSO bands, a QD band (8-to-12 years), and a multi-decadal band (18-to-60 years). Significance of peaks within bands is obtained after polynomial smoothing and bootstrapping procedures. Datasets have been redistributed by keeping their spatial locations, while time-series for each individual month were being randomly permuted 1000 times and re-analyzed using same method. This procedure minimized bias from serial correlation in the model, kept spatial structures intact and preserved degrees of freedom. The confidence levels (%) obtained from Monte-Carlo simulation are displayed in Figure 1.

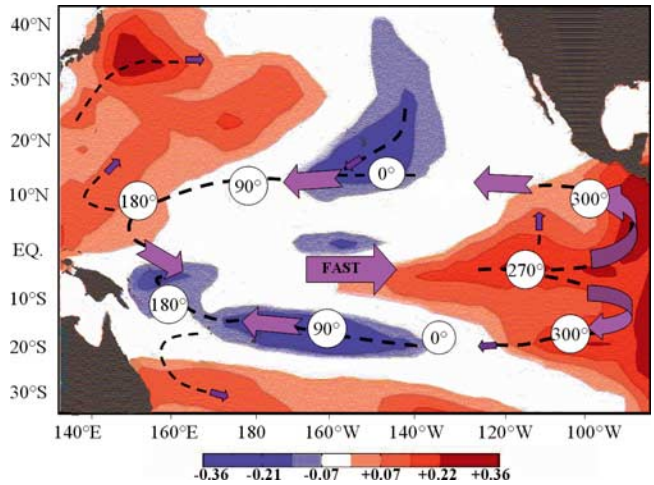

Figure 2. Quasi-decadal (0.1 cycle/year, or QD) snapshot of SST anomalies (for the arbitrary 270° phase, when maximum anomalies are found straddling the equator). Purple arrows indicate directions along main trajectories (thick dashed lines) followed by thermal anomalies associated with QD fluctuations. Other QD phases along pathways are within circles. Colored scale is in °C anomalies (negative in blue; positive in red).

[8] In the lower-frequency part of the spectrum, QD fluctuations peak at 0.1cycle/year while within the multi-decadal band, ID fluctuations (i.e., 18-to-25 years) peak at ~0.04 cycle/year. A significant penta-decadal fluctuation (40-to-60 years) is also noticeable. To shed more light on associated physical mechanisms, reconstructed spatial evolutions for QD and ID signals are reproduced in Figures 2 and 3, respectively.

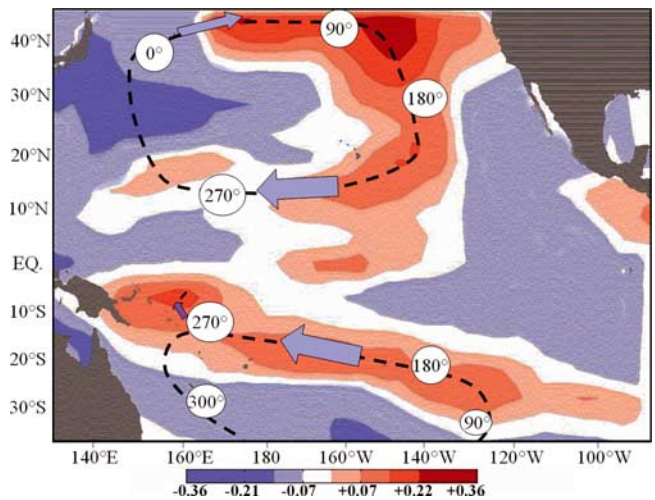

Figure 3. Inter-decadal (0.04 cycle/year, or ID) snapshot of SST anomalies (for the arbitrary 90° phase, when maximum anomalies are in the eastern part of the northern gyre). Other ID phases are within circles. Colored scale is in °C anomalies. Purple arrows along thick dashed lines represent main trajectories followed by thermal anomalies associated with the fluctuation.

[9] During the modeled QD evolution (Figure 2), coherent spatial patterns of SSTA of a given polarity are found evolving from the east-northeast and southeast Pacific into the western tropics. The SSTA displayed in Figure 2, is a snapshot (i.e., for the arbitrary 270° phase). If we start at phase 0° between 130°W and 150°W in the northern and southern hemispheres, a slow westward evolution at ~15°N and 15°S follows and it takes about 5 years to go from the tropical eastern Pacific into the western tropics (~180° phase). During that period maximum SSTA are found in the southwest Pacific where maximum variability in the σ_θ = 25 isopycnal is found (~90° phase) which modifies upper-layers heat content. Then quite rapidly, maximum SSTA of the same polarity are found almost straddling the central/eastern equatorial Pacific (~270° phase) with maxima slightly south of the equator, leading to patterns resembling ENSO warm/cold equatorial phases. Subsequently, reflections of SSTA occur along the eastern boundaries, with evidence of slow westward propagation away from the equator (phases 270° to 0°/360°). Moreover, the spatial evolution of SLPA is such that SSTA and SLPA with same polarity develop together in the north Pacific (arbitrary phase 0°, not shown). From phases 180° to 270°, SLPA are found over the anticyclonic gyre enhancing/slowing-up SSTA evolution (not shown). Phase 270° is also the time when the QD variability of the Southern Oscillation Index (SOI) should weaken equatorial easterlies and be associated with low-frequency ENSO warm phases.

[10] During the modeled ID evolution (Figure 3), maximum SSTA propagate clockwise and counter-clockwise along the subtropical gyres in both Northern and Southern Hemispheres, respectively. In the Northern Hemisphere, maximum SSTA can be found first near the SAFZ, where Newtonian damping from surface fluxes limits extent of SST anomalies thus introducing ID type fluctuations and then along the subtropical gyre [*Seager et al.*, 2001]. SSTA can be traced into the Philippines Seas. Anomalies then propagate poleward along the western boundaries of the Northern Hemisphere, different to what has been observed [*Tourre et al.*, 1999]. Tropical maximum SSTA of the same polarity are found away from the equator. SLPA associated with modeled ID fluctuations (not shown) develop in the northeast Pacific well before SSTA (~3–4 years) of the same polarity are identified northeast of the SAFZ.

4. Discussion and Conclusion

[11] Recently, QD and ID variability in the Pacific Ocean have been identified as two different phenomena [*Tourre et al.*, 2001]. Here, climate fluctuations in the Pacific Ocean have been investigated using a 200-year simulation from the ARPEGE-Climat/ORCA2 coupled models at CERFACS. Spatio-temporal evolution of the statistically distinct QD and ID fluctuations are compared to that from diagnostic studies. Insight on physical mechanisms from CGCM is given hereafter.

[12] For the modeled QD fluctuations, thermal anomalies are found off the equator propagating slowly westward from the eastern Pacific, with phase velocities comparable to that of coupled Rossby waves (~5 cm/s at 15°N and 15°S), compatible with results from *Capotondi and Alexander* [2001]. After reflection along the western boundaries, fast equatorial eastward propagation of thermal anomalies follows. This leads to rapid equatorial warm/cold events at the surface in the central/eastern Pacific. The evolution of QD upper ocean heat content anomalies evidenced at the equator and lag-regression analysis between the zonal wind stress and depth of the 20°C isotherm (not shown), suggest that recharge/discharge mechanisms could be at work as in *Hasegawa and Hanawa* [2003]. The phase velocity for equatorial propagation of subsurface thermal anomalies is different (faster) than that of the delayed oscillator as in *White et al.* [2003]. In the Southern Hemisphere, the QD SST variability is associated with local changes in wind-stress curl and adiabatic displacement of the thermocline (from Ekman pumping, between 100 and 150 meters) rather than anomalous advection of spiciness anomalies [*Schneider*, 2000]. It resembles the thermal ocean evolution identified by *Luo and Yamagata* [2001] and *Bratcher and Giese* [2002], with a slightly shorter period (i.e., 8-to-12 years instead of 14 years). Additional analyses show that influence of heat and fresh water fluxes appears to be weak in the southwest Pacific on this time scale. From the above, the QD fluctuations can then be seen as a low-frequency ENSO, thus changing the 'classic' ENSO band-period (i.e., 3-to-8 years) into an extended 3-to-12 years band-period. This is a different view from a low-frequency modulation of ENSO, as proposed by *Timmermann* [2003] and *Rodgers et al.* [2004]. Finally, results also suggest asymmetry between equatorial events, adding to the non-linearities of the equatorial system which could also contribute to equatorial QD fluctuations. This requires further testing of the model.

[13] For the modeled ID fluctuations, SSTA follow the path of upper-ocean heat content [*Zhang and Levitus*, 1997; *Hasegawa*, 2003], and can be traced all the way from the SAFZ region into the subtropical gyre and then into the western Pacific. For unidentified reasons, subduction processes in the model are less than that observed [*Deser et al.*, 1996; *Tourre et al.*, 1999], since advected SSTA remain at the surface in the southern part of the gyre. Additional mechanisms on possible oceanic origin/negative feedback of ID fluctuations remains to be tested. While there is little evidence of reflection along the western boundaries as observed, maximum SSTA in the central Pacific and away from the equator could modulate tropical thermal background [*Barnett et al.*, 1999], intensity and frequency of ENSO [*Wang*, 1995; *Kleeman et al.*, 1999; *White and Cayan*, 2000]. This also requires further investigation.

[14] This study illustrates the ability of a CGCM to reproduce low-frequency variability in the Pacific with distinct signals and physics. While this variability is supposedly less dependent on the mean state of the model, a better representation of its seasonal variability could have impacts on ENSO characteristics (Dewitte et al., submitted manuscript, 2004). While the equatorial recharge/discharge mechanism [*Jin*, 1997] seems to operate at decadal time scale, further testing such as that of *An and Jin* [2001], suggests more complex vertical structure variability of wave dynamics particularly at mid-latitudes [*Liu*, 1999; *Thompson and Ladd*, 2004]. The latter show that the first three baroclinic modes in the northern Pacific seem to be

forced by the atmosphere only. Overall results corroborate the use of CGCM for studying low-frequency signals and their linkages with ENSO as that of *Yeh and Kirtman* [2004]. This study provides additional theoretical background for further analyses and interpretation of the low-frequency modes from the CGCM.

[15] **Acknowledgments.** Yves M. Tourre would like to thank Dr. Jean-Claude André, Director of CERFACS for facilitating and encouraging this research. Appreciation is extended to Eric Fourlon, responsible for installing the MTM/SVD code at MEDIAS-France. Thanks also to Dr. Gérard Bégni Director of MEDIAS-France and Dr. Arnold Gordon, Head of Physical Oceanography at LDEO of Columbia University. This is LDEO contribution # 6737.

References

An, S.-I., and F.-F. Jin (2001), Collective role of thermocline and zonal advective feedbacks in the ENSO mode, *J. Clim.*, *14*, 3421–3432.

Auad, G. (2003), Interdecadal dynamics of the North Pacific Ocean, *J. Phys. Oceanogr.*, *33*, 2483–2503.

Barnett, T. P., D. W. Pierce, M. Latif, D. Dommenget, and R. Saravanan (1999), Interdecadal interactions between the tropics and midlatitudes in the Pacific basin, *Geophys. Res. Lett.*, *26*, 615–618.

Bratcher, A. M., and B. S. Giese (2002), Tropical Pacific decadal variability and global warming, *Geophys. Res. Lett.*, *29*(19), 1918, doi:10.1029/2002GL015191.

Capotondi, A., and M. A. Alexander (2001), Rossby waves in the tropical North Pacific and their role in decadal thermocline variability, *J. Phys. Oceanogr.*, *31*, 3496–3515.

Cibot, C., E. Maisonnave, L. Terray, and B. Dewitte (2005), Mechanisms of tropical Pacific interannual-to-decadal variability in the ARPEGE/ORCA global coupled model, *Clim. Dyn.*, in press.

Deser, C., A. Alexander, and M. S. Timlin (1996), Upper-ocean thermal variations in the North Pacific during winter: 1900–1989, *J. Clim.*, *9*, 1840–1855.

Hasegawa, T. (2003), Upper ocean heat content variability in the Pacific Ocean, Ph.D. thesis, Dep. of Geophys., 156 pp., Tohoku Univ., Sendai, Japan.

Hasegawa, T., and K. Hanawa (2003), Decadal-scale variability of upper ocean heat content in the tropical Pacific, *Geophys. Res. Lett.*, *30*(6), 1272, doi:10.1029/2002GL016843.

Jin, F. F. (1997), An equatorial ocean recharge paradigm for ENSO. Part I: Conceptual model, *J. Atmos. Sci.*, *54*, 811–829.

Kachi, M., and T. Nitta (1997), Decadal variations of the global atmosphere-ocean system, *J. Meteorol. Soc. Jpn.*, *75*, 657–675.

Kaplan, A., M. Cane, Y. Kushnir, A. Clement, B. Blumenthal, and B. Rajagopalan (1998), Analyses of global sea surface temperature 1856–1991, *J. Geophys. Res.*, *103*, 18,567–18,589.

Kirtman, B. P., and P. S. Schopf (1998), Decadal variability in ENSO predictability and prediction, *J. Clim.*, *11*, 2804–2822.

Kleeman, R., J. McCreary, and B. Klinger (1999), A mechanism for generating ENSO decadal variability, *Geophys. Res. Lett.*, *26*, 1743–1746.

Latif, M., and T. Barnett (1994), Causes of decadal climate variability over the North Pacific and North America, *Science*, *266*, 634–637.

L'Heureux, M. L., M. E. Mann, B. I. Cook, B. E. Gleason, and R. Vose (2004), Atmospheric circulation influences on seasonal precipitation patterns in Alaska during the latter 20th century, *J. Geophys. Res.*, *109*, D06106, doi:10.1029/2003JD003845.

Liu, Z. (1999), Forced planetary waves response in a thermocline gyre, *J. Phys. Oceanogr.*, *29*, 1036–1055.

Luo, J., and T. Yamagata (2001), Long-term El Niño–Southern Oscillation (ENSO)-like variation with special emphasis on the South Pacific, *J. Geophys. Res.*, *106*, 22,211–22,228.

Mantua, N. J., S. R. Hare, Y. Zhang, J. M. Wallace, and R. C. Francis (1997), A Pacific interdecadal climate oscillation with impacts on salmon production, *Bull. Am. Meteorol. Soc.*, *78*, 1069–1079.

Miller, A. J., and N. Schneider (2000), Interdecadal climate regime dynamics in the North Pacific Ocean: Theories, observations and ecosystems impacts, *Prog. Oceanogr.*, *47*, 355–379.

Mann, M. E., and J. Park (1999), Multivariate signal detection in climate studies, *Adv. Geophys.*, *41*, 1–131.

Pierce, D. W., T. P. Barnett, N. Schneider, R. Saravanan, D. Domenget, and M. Latif (2001), The role of ocean dynamics in producing decadal climate variability in the North Pacific, *Clim. Dyn.*, *18*, 51–70.

Qiu, B. (2003), Kuroshio extension variability and forcing of the Pacific decadal oscillations: Responses and potential feedback, *J. Phys. Oceanogr.*, *33*, 2465–2482.

Rodgers, K., P. Friederichs, and M. Latif (2004), Tropical Pacific decadal variability and its relation to decadal modulations of ENSO, *J. Clim.*, *17*, 3761–3774.

Schneider, N. (2000), A decadal spiciness mode in the tropics, *Geophys. Res. Lett.*, *27*, 257–260.

Seager, R., Y. Kushnir, N. H. Naik, M. A. Cane, and J. Miller (2001), Wind-driven shifts in the latitude of the Kuroshio-Oyashio extension and generation of SST anomalies on decadal timescales, *J. Clim.*, *14*, 4249–4265.

Sekine, Y. (1988), Anomalous southward intrusion of the Oyashio east of Japan: 1. Influence of the seasonal and interannual variations in the wind stress over the North Pacific, *J. Geophys. Res.*, *93*, 2247–2255.

Thompson, L. A., and C. A. Ladd (2004), The response of the North Pacific Ocean to decadal variability in atmospheric forcing: Wind versus buoyancy forcing, *J. Phys. Oceanogr.*, *34*, 1373–1386.

Timmermann, A. (2003), Decadal ENSO amplitude modulations: A nonlinear paradigm, *Global Planet. Change*, *37*, 135–156.

Tourre, Y. M., Y. Kushnir, and W. B. White (1999), Evolution of interdecadal variability in sea level pressure, sea surface temperature, and upper ocean temperature over the Pacific Ocean, *J. Phys. Oceanogr.*, *9*, 1528–1541.

Tourre, Y. M., B. Rajagopalan, Y. Kushnir, M. Barlow, and W. B. White (2001), Patterns of coherent ocean decadal and interdecadal climate signals in the Pacific basin during the 20th century, *Geophys. Res. Lett.*, *28*, 2069–2072.

Wang, B. (1995), Interdecadal changes in El Niño onset in the last four decades, *J. Clim.*, *8*, 267–285.

White, W. B., and D. R. Cayan (2000), A global ENSO wave in surface temperature and pressure and its interdecadal modulation from 1900 to 1997, *J. Geophys. Res.*, *105*, 11,223–11,242.

White, W. B., Y. M. Tourre, M. Barlow, and M. Dettinger (2003), A delayed action oscillator shared by biennial, interannual, and decadal signals in the Pacific Basin, *J. Geophys. Res.*, *108*(C3), 3070, doi:10.1029/2002JC001490.

Yeh, S., and B. P. Kirtman (2004), Tropical Pacific decadal variability and ENSO amplitude modulation in a CGCM, *J. Geophys. Res.*, *109*, C11009, doi:10.1029/2004JC002442.

Zhang, R. H., and S. Levitus (1997), Structure and cycle of decadal variability of upper-ocean temperature in the North Pacific, *J. Clim.*, *10*, 710–727.

C. Cibot, Météo-France, 42, Avenue Gaspard Coriolis, F-31057 Toulouse Cedex 01, France.

B. Dewitte, LEGOS/IRD, 18, Avenue Edouard Belin, F-31401 Toulouse, France.

L. Terray, Centre Européen de Recherche et de Formation Avancée en Calcul Scientifique (CERFACS), 42, Avenue Gaspard Coriolis, F-31057 Toulouse Cedex 01, France.

Y. M. Tourre, MEDIAS-France, Centre National d'Etudes Spatiales, Bpi 2102, 18 Avenue Edouard Belin, F-31401 Toulouse Cedex 9, France. (tourre@medias.cnes.fr)

W. B. White, Scripps Institution of Oceanography, University of California San Diego, 9500 Gilman Drive, La Jolla, CA 92093-0233, USA.